OVERLAPPING SCHWARZ METHODS FOR FEKETE AND GAUSS–LOBATTO SPECTRAL ELEMENTS[*]

L. F. PAVARINO[†], E. ZAMPIERI[†], R. PASQUETTI[‡], AND F. RAPETTI[‡]

Abstract. The classical overlapping Schwarz algorithm is here extended to the triangular/tetrahedral spectral element (TSEM) discretization of elliptic problems. This discretization, based on Fekete nodes, is a generalization to nontensorial elements of the tensorial Gauss–Lobatto–Legendre quadrilateral spectral elements (QSEM). The overlapping Schwarz preconditioners are based on partitioning the domain of the problem into overlapping subdomains, solving local problems on these subdomains, and solving an additional coarse problem associated with either the subdomain mesh or the spectral element mesh. The overlap size is generous, i.e., one element wide, in the TSEM case, while it is minimal or variable in the QSEM case. The results of several numerical experiments show that the convergence rate of the proposed preconditioning algorithm is independent of the number of subdomains N and the spectral degree p in case of generous overlap; otherwise it depends inversely on the overlap size. The proposed preconditioners are also robust with respect to arbitrary jumps of the coefficients of the elliptic operator across subdomains.

Key words. spectral elements, Fekete nodes, Gauss–Lobatto–Legendre nodes, overlapping Schwarz preconditioners

AMS subject classifications. 65N55, 65N35, 65F10

DOI. 10.1137/060663568

1. Introduction. Spectral and hp-finite elements are among the most successful high-order methods for the numerical approximation of partial differential equations. These methods can achieve spectral convergence of the discrete solution by allowing both h-refinement of the elements mesh and p-refinement of the polynomial degree in each element. While hierarchical hp-finite elements employ modal basis functions (see [29, 27]), spectral element methods on quadrilateral elements (QSEM) employ a nodal approach based on the tensorial product of one-dimensional Gauss–Lobatto–Legendre (GLL) points (see, e.g., [1, 17, 7]). The need to extend spectral element formulations to complex geometries and unstructured meshes has recently led to the construction and study of triangular/tetrahedral spectral elements (TSEM); see, e.g., [15, 16, 31, 33, 12, 13] and the previous studies of interpolation nodes on triangles [5, 6, 14] and on p-version substructuring methods [2]. In this paper, we consider TSEM based on the Fekete nodes [3, 30], as in our previous works [19, 20, 21].

The discrete systems produced by these high-order methods are much more ill-conditioned than in the standard finite element or finite difference cases, and therefore the design and analysis of efficient iterative solvers is still a challenging research topic. In this paper, we construct and study overlapping Schwarz methods for Fekete–Gauss TSEM, obtaining solvers that are scalable (independent of the number of subdomains N) and optimal (independent of the spectral degree p). This last property holds because we employ generous overlap (at least one element wide) between subdomains. In the QSEM case it is possible to construct Schwarz preconditioners with minimal

[†]Department of Mathematics, Università di Milano, Via Saldini 50, 20133 Milan, Italy (Luca.Pavarino@mat.unimi.it, Elena.Zampieri@mat.unimi.it).

[‡]Laboratoire J.-A. Dieudonné, CNRS & Université de Nice et Sophia-Antipolis, Parc Valrose, 06108 Nice cedex 02, France (rpas@math.unice.fr, frapetti@math.unice.fr).

overlap by extending each subdomain with a few rows of GLL nodes of the neighboring elements [4, 10, 11, 18], but the design of a similar technique in the TSEM case is still an open problem, since Fekete points are not distributed as a tensor product. The good convergence properties of our solver are retained also for heterogeneous problems with discontinuous coefficients across subdomain boundaries. Preliminary results with only one element per subdomain and constant coefficients have been reported in the conference paper [21]. A different approach involving preconditioners based on nonoverlapping methods of Neumann–Neumann type for TSEM has been recently studied in [22].

In the rest of the paper, we introduce the model elliptic problem and its QSEM and TSEM discretizations (section 2), the overlapping Schwarz preconditioners in additive and multiplicative form (section 3), and the results of several numerical experiments with the additive Schwarz preconditioners for TSEM and QSEM for homogeneous and heterogeneous problems (section 4).

2. The model problem and SEM formulation. Let $\Omega \in \mathbb{R}^d$, $d = 2, 3$, be a bounded Lipschitz domain with piecewise smooth boundary $\partial\Omega$. For simplicity, we consider a model elliptic problem in the plane ($d = 2$), with homogeneous Dirichlet boundary data, but the numerical methods and results presented in this paper can be applied equally well in three dimensions and to more general elliptic problems:

$$(2.1) \qquad -\mathrm{div}(\alpha \,\mathbf{grad}\, u) + \beta u = f \quad \text{in } \Omega, \qquad u = 0 \quad \text{on } \partial\Omega,$$

where α, $\beta > 0$ are piecewise constant in Ω and f is a given function in $L^2(\Omega)$. We denote by $L^2(\Omega)$ the space of square integrable measurable functions in Ω, and by $H^1(\Omega)$ the space of functions in $L^2(\Omega)$ whose gradient is in $[L^2(\Omega)]^2$. Then let V be the Sobolev space

$$V \equiv H_0^1(\Omega) = \{v \in H^1(\Omega) : v = 0 \text{ on } \partial\Omega\}.$$

The weak formulation of (2.1) reads (see, e.g., [26]): Find $u \in V$ such that

$$(2.2) \qquad a(u, v) := \int_\Omega (\alpha \mathbf{grad} u \cdot \mathbf{grad} v + \beta \, u \, v) \, \mathrm{d}\mathbf{x} = (f, v) := \int_\Omega f \, v \, \mathrm{d}\mathbf{x} \quad \forall v \in V.$$

The variational problem (2.2) is discretized by the standard conforming spectral element method, either quadrilateral-based (QSEM) or triangle-based (TSEM). The method can be viewed as a nodal version of the hp-finite element method, which uses GLL points of the quadrilateral for the QSEM and the Fekete points of the triangle for the TSEM, and employs a discrete space consisting of continuous piecewise polynomials of degree p within each quadrilateral or triangular spectral element; see [1, 7, 17] for a general introduction and an analysis of the method. For the QSEM, let Q_{ref} be the reference square $(-1, 1)^2$ and let $\mathbb{Q}_p(Q_{\mathrm{ref}})$ be the set of polynomials on Q_{ref} of degree $\leq p$ in each variable. Then, for the TSEM, let $T_{\mathrm{ref}} = \{(r, s) : -1 \leq r, s, \ r + s \leq 0\}$ be the reference triangle and let $\mathbb{P}_p(T_{\mathrm{ref}})$ be the set of polynomials on T_{ref} of total degree $\leq p$. We assume that the original domain Ω is decomposed into K quadrilateral or triangular spectral elements T_k,

$$\overline{\Omega} = \bigcup_{k=1}^K \overline{T}_k.$$

This is a conforming finite element partition; in particular, the intersection between two distinct elements T_k is either the empty set or a common vertex or a common side.

We denote by h the maximum diameter of the elements T_k and by τ_h the associated finite element mesh. Each element T_k is the image of the reference square Q_{ref} or triangle T_{ref} by means of a suitable mapping g_k, $k = 1, \ldots, K$, i.e., $T_k = g_k(Q_{\text{ref}})$ or $T_k = g_k(T_{\text{ref}})$.

Finally, the space V is discretized by continuous piecewise polynomials of degree $\leq p$ in each variable for QSEM,

$$V_{K,p}^Q = \{v \in V : v|_{\Omega_k} \circ g_k \in \mathbb{Q}_p(Q_{\text{ref}}), \ k = 1, \ldots, K\},$$

or of total degree $\leq p$ for TSEM,

$$V_{K,p}^T = \{v \in V : v|_{\Omega_k} \circ g_k \in \mathbb{P}_p(T_{\text{ref}}), \ k = 1, \ldots, K\}.$$

The spectral element approximation of the variational elliptic problem (2.2) is obtained by replacing the L^2-inner product and the bilinear form defined in (2.2) with their approximations based either on GLL points for QSEM or on Gauss points for the Fekete–Gauss TSEM.

2.1. The GLL QSEM. We consider conforming QSEM based on GLL quadrature points, which also allows the construction of a tensor-product basis for $V_{K,p}^Q$. We denote by $\{\xi_j\}_{j=0}^p$ the set of GLL points of $[-1, 1]$ that are the $(p+1)$ zeros of the polynomial

$$(1 - \zeta^2)\frac{\partial L_p(\zeta)}{\partial \zeta},$$

where L_p is the pth Legendre polynomial in $[-1, 1]$. Then we denote by σ_j the quadrature weight associated with ξ_j. Let $l_j(x)$ be the Lagrange interpolating polynomial of degree $\leq p$ which vanishes at all the GLL nodes except ξ_j, where it equals 1. The Lagrangian nodal basis functions on the reference square Q_{ref} are defined by building tensor products

$$l_j(x)l_\ell(y), \quad 0 \leq j, \ell \leq p.$$

Each function $u \in \mathbb{Q}_p(Q_{\text{ref}})$ is expanded in this nodal GLL basis through its values at GLL nodes $u(\xi_j, \xi_\ell)$, $0 \leq j, \ell \leq p$, as

$$u(x, y) = \sum_{j=0}^p \sum_{\ell=0}^p u(\xi_j, \xi_\ell)l_j(x)l_\ell(y).$$

Then, on Q_{ref}, the discrete L^2-inner product is

$$(u, v)_{Q_{\text{ref}}, p} = \sum_{j=0}^p \sum_{\ell=0}^p u(\xi_j, \xi_\ell)v(\xi_j, \xi_\ell)\sigma_j\sigma_\ell,$$

and in general on Ω,

$$(2.3) \qquad (u, v)_{K,p}^Q = \sum_{k=1}^K \sum_{j,\ell=0}^p (u \circ g_k)(\xi_j, \xi_\ell)(v \circ g_k)(\xi_j, \xi_\ell)|J_k^Q|\sigma_j\sigma_\ell,$$

where $|J_k^Q|$ is the Jacobian of the mapping g_k. We then obtain the discrete variational problem: Find $u \in V_{K,p}^Q$ such that

$$(2.4) \qquad a_{K,p}^Q(u, v) = (f, v)_{K,p}^Q \quad \forall v \in V_{K,p}^Q,$$

where $a_{K,p}^Q(\cdot, \cdot)$ is obtained by substituting each integral in (2.2) with the GLL quadrature rule (2.3).

The discrete problem (2.4) can be written equivalently in matrix form as a linear system $A_Q \mathbf{u} = \mathbf{b}$, where A_Q is here the assembled QSEM matrix, $\mathbf{b}$ is the load vector accounting for the contribution of f, and $\mathbf{u}$ is the vector of the unknown nodal values of the function u at the GLL nodes.

2.2. The Fekete–Gauss TSEM. For TSEM it is no longer possible to define spectral elements by tensor product as for QSEM. With $n = (p + 1)(p + 2)/2$, let $\{\psi_j\}_{j=1}^n$ be a polynomial basis of $\mathbb{P}_p(T_{\mathrm{ref}})$ for the usual $L^2(T_{\mathrm{ref}})$-inner product, e.g., the Koornwinder–Dubiner orthogonal basis [9]. The Fekete points on T_{ref} are defined as the points $\{\hat{\mathbf{x}}_i\}_{i=1}^n$ that maximize the determinant of the Vandermonde matrix V with elements

$$V_{ij} = \psi_j(\hat{\mathbf{x}}_i), \quad 1 \le i, j \le n,$$

and an algorithm to accurately solve the corresponding optimization problem is described in [30]. For TSEM introduced in [31], the Fekete points are used as approximation points; i.e., the Lagrange polynomials $\{\phi_i\}_{i=1}^n$ built on these points are used as basis functions. Among the main properties of Fekete points proved in [3, 30], we recall that for the cube, Fekete points and Gauss–Lobatto points coincide, thus providing a strong link with the usual QSEM.

Unlike GLL points, a quadrature formula based on Fekete points is exact only for integrands in $\mathbb{P}_p(T_{\mathrm{ref}})$. This fact has suggested for the TSEM that we might separate the sets of approximation and quadrature points, using the Fekete points $\{\hat{\mathbf{x}}_i\}_{i=1}^n$ for the first set and Gaussian points $\{\hat{\mathbf{y}}_i\}_{i=1}^m$ for the second set, obtained by imposing an exact integration of polynomials, e.g., in $\mathbb{P}_{2p}(T_{\mathrm{ref}})$; see [20]. Given the values of a polynomial $u_p \in \mathbb{P}_p(T_{\mathrm{ref}})$ at the Fekete points, one can set up interpolation and differentiation matrices to compute, at the Gauss points, the values of u_p and of its derivatives, respectively. For instance, denoting by $\underline{u}$ the vector of the $u_i = u_p(\hat{\mathbf{x}}_i)$, $1 \le i \le n$, and by $\underline{u}'$ that of the $u_p(\hat{\mathbf{y}}_i)$, $1 \le i \le m$, we have $\underline{u}' = V'V^{-1}\underline{u}$, where $V'_{ij} = \psi_j(\hat{\mathbf{y}}_i)$. On a generic triangle $T_k = g_k(T_{\mathrm{ref}})$, the same relation between $\underline{u}'$ and $\underline{u}$ holds true, provided that $u_i = (u_p \circ g_k)(\hat{\mathbf{x}}_i)$ and $u'_j = (u_p \circ g_k)(\hat{\mathbf{y}}_j)$. Similarly, in T_{ref} one has $(\partial \underline{u})' = W'V^{-1}\underline{u}$, with ∂ for differentiation with respect to any coordinates and where $W'_{ij} = \partial\psi_j(\hat{\mathbf{y}}_i)$. Then, using the chain rule, one can compute derivatives in the generic triangle.

The TSEM requires, of course, the use of highly accurate integration rules based on Gauss points, which are still an open subject of research, but in any case, we can use integration rules based on Gauss points for the quadrilateral and then map them to T_{ref}; see [17]. On a generic triangle $T_k = g_k(T_{\mathrm{ref}})$,

$$(u, v)_{T_k, p} = \sum_{j=1}^m u'_j \, v'_j \, |J_k^T(\hat{\mathbf{y}}_j)| \, \omega_j,$$

where $\omega_j > 0$, $1 \le j \le m$, are the quadrature weights and $|J_k^T|$ is the Jacobian of the mapping g_k between T_{ref} and T_k, and in general on Ω,

$$(2.5) \qquad (u, v)_{K, p}^T = \sum_{k=1}^K (u, v)_{T_k, p}.$$

As for (2.4), we obtain a discrete problem

$$(2.6) \qquad a_{K,p}^T(u,v) = (f,v)_{K,p}^T \quad \forall v \in V_{K,p}^T,$$

which can be written in matrix form as a linear system $A_T \mathbf{u} = \mathbf{b}$. The TSEM matrix A_T is less sparse than the QSEM matrix A_Q and more ill-conditioned, since its condition number grows as $O(p^4 h^{-2})$ rather than $O(p^3 h^{-2})$ for $d = 2$ (see section 4).

3. Decomposition into subdomains and overlapping Schwarz precon-ditioners. We now apply some domain decomposition techniques and build some preconditioning techniques for the iterative solution of the QSEM or TSEM discrete systems $A\mathbf{u} = \mathbf{b}$ by the preconditioned CG (PCG) method, with $A = A_Q$ for QSEM or $A = A_T$ for TSEM. The preconditioner belongs to the family of over-lapping Schwarz methods and is built from the solution of parallel independent local elliptic problems on overlapping subdomains, in addition to the solution of coarse problems on the coarse mesh, needed to ensure scalability. For a general introduction to domain decomposition methods and overlapping Schwarz preconditioners we refer to [8, 32, 28, 26] and the references therein.

Preliminary results on overlapping Schwarz preconditioners for Fekete TSEM have been reported in the conference paper [21], where we considered only the case of one spectral element per subdomain and constant coefficients in the elliptic operator. For the classical GLL QSEM case with only one element per subdomain, several works are available in the literature, both for the scalar and vector cases; see, e.g., [4, 10, 24, 25]. In this paper, we extend our investigation to the more general case where Ω is decomposed into subdomains Ω_i, which are in turn partitioned into spectral elements, for both the triangular and quadrilateral case. To this aim, we assemble the elements T_k, $k = 1, \ldots, K$, of the QSEM or TSEM partitions into N quadrilateral or triangular subdomains Ω_i, each consisting of K_i spectral elements T_k. With a local renumbering of the triangles we then have

$$\overline{\Omega}_i = \bigcup_{k=1}^{K_i} \overline{T}_k,$$

where $K = \sum_i K_i$ (see Figures 1–3 below for some examples). We assume also that the subdomain partition is conforming, i.e., that the intersection between two distinct subdomains is either the empty set or a common vertex or a common side, and we denote by H the maximum diameter of the subdomains Ω_i.

The coarse mesh τ_0 is defined to be either the subdomain mesh τ_H or the element mesh τ_h. Let τ_p be the fine discretization mesh determined by either the GLL or the Fekete nodes introduced in each element T_k in sections 2.1 and 2.2. We can define different discretizations and overlapping partitions, according to the spectral element domain decomposition of Ω and the set of nodes within each subdomain. In the special case where $H = h$, each element T_k coincides with a whole subdomain. When $H > h$, we associate groups of triangular or quadrilateral elements to each subdomain, and two different choices for the coarse problem are possible, one associated with the subdomain mesh τ_H, the other with the element mesh τ_h, and both using coarse basis functions with $p = 1$ polynomial degree. We will denote them as τ_H-coarse space and τ_h-coarse space.

QSEM. The coarse triangulation τ_0 is given by quadrilateral subdomains Ω_i (resp., elements T_k) providing a coarse problem on $\tau_0 \equiv \tau_H$ (resp., $\tau_0 \equiv \tau_h$) with bilinear finite
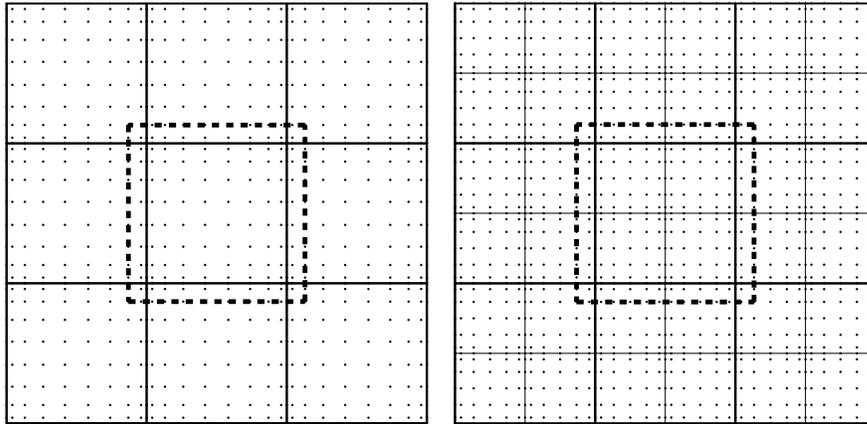
FIG. 1. *QSEM examples with $N = 3 \times 3$ subdomains Ω_i' corresponding to an overlap of $\delta = 2$ GLL points. The internal overlapping subdomain is depicted with thick dashed lines. Left: spectral degree $p = 9$ and $K_i = 1$; i.e., each subdomain consists of only one element. Right: spectral degree $p = 6$ and $K_i = 2 \times 2$; i.e., each subdomain consists of four elements.*

elements ($p = 1$ in each direction). Then the local fine discretization τ_p is determined by GLL nodes in each subdomain Ω_i, when we associate each quadrilateral finite element to a subdomain, or GLL nodes in each element T_k, when each subdomain Ω_i is in turn partitioned into K_i quadrilateral elements of smaller size h. We observe that τ_p is not shape-regular, because the distance between GLL points close to the endpoints of $[-1, 1]$ is on the order of $1/p^2$, while in the middle of the interval $[-1, 1]$ this distance is on the order of $1/p$ (see [1]).

We consider an overlapping partition of Ω by extending each subdomain Ω_i to a larger subdomain Ω_i', consisting of all GLL nodes of τ_p within a certain distance δ^* from Ω_i. Precisely, $\delta^* = \min_{i=1}^{N} \{\text{dist}(\partial\Omega_i, \partial\Omega_i')\}$. We also measure the size of the overlapping region by the number δ of GLL points extending Ω_i in each direction. For example, in the case of minimal overlap and a uniform partition of a square domain Ω, as in Figure 1, we have $\delta = 1$ and $\delta^* = (\xi_1 - \xi_0)h/2$, where ξ_0 and ξ_1 are respectively the first and second GLL node in $[-1, 1]$; in the case of generous overlap we have $\delta = p$ and $\delta^* = h$.

See Figure 1 (left) for a two-dimensional example on a square domain Ω corresponding to local polynomial degree $p = 9$ and one element per subdomain ($H = h$), and Figure 1 (right) for a two-dimensional example on a square domain Ω corresponding to local polynomial degree $p = 6$ and $K_i = 2 \times 2$ elements per subdomain ($H = 2h$). In both cases the original domain Ω is decomposed into $N = 3 \times 3$ subdomains, with overlap $\delta = 2$ GLL points.

TSEM. The coarse triangulation τ_0 is given either by all quadrilateral or triangular subdomains Ω_i, providing a coarse problem on $\tau_0 \equiv \tau_H$ with, respectively, bilinear or linear finite elements ($p = 1$), or by all triangular elements T_k providing a richer coarse problem on $\tau_0 \equiv \tau_h$ with linear finite elements ($p = 1$). Then the local fine discretization τ_p is determined by Fekete nodes within each subdomain Ω_i in the first case, or within each element T_k in the second one. The overlapping partition of Ω is generated by extending each quadrilateral or triangle Ω_i to a large subdomain Ω_i' consisting of all triangular elements sharing with Ω_i either a vertex or an edge. See Figure 2 for a two-dimensional example on a square domain Ω corresponding to
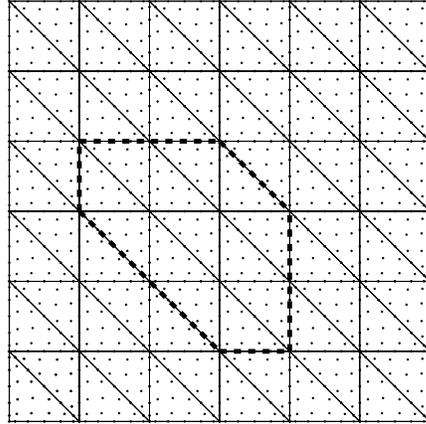
FIG. 2. *TSEM example with spectral degree $p = 6$, $K = 6 \times 6 \times 2$ triangular elements, and $K_i = 1$; i.e., each subdomain consists of only one element. In this case, an internal overlapping subdomain (depicted with thick dashed lines) consists of 13 elements.*
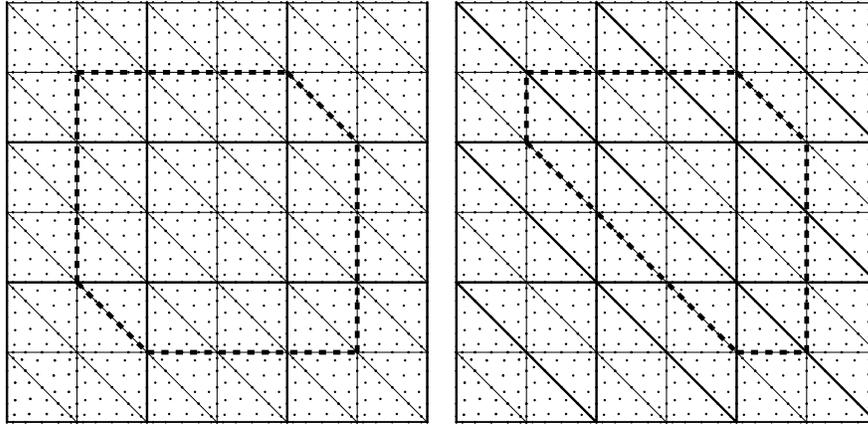
FIG. 3. *TSEM example with spectral degree $p = 6$. Left: $N = 3 \times 3$ square subdomains, $K_i = 2 \times 2 \times 2$ elements per subdomain; in this case, an internal overlapping subdomain (depicted with thick dashed lines) consists of 30 elements. Right: $N = 3 \times 3 \times 2$ triangular subdomains, $K_i = 4$ elements per subdomain; in this case, an internal overlapping subdomain (depicted with thick dashed lines) consists of 22 elements.*

$N = 6 \times 6 \times 2$ triangular subdomains ($H = 1/3$), polynomial degree $p = 6$, and one element per subdomain ($H = h$). Moreover, see Figure 3 (left) for a two-dimensional example corresponding to $N = 3 \times 3$ quadrilateral subdomains ($H = 2/3$), polynomial degree $p = 6$, and $K_i = 2 \times 2 \times 2$ triangular elements per subdomain, and Figure 3 (right) for a two-dimensional example corresponding to $N = 3 \times 3 \times 2$ triangular subdomains, polynomial degree $p = 6$, and $K_i = 2 \times 2$ triangular elements per subdomain. Overlapping techniques involving a smaller number of elements (e.g., sharing edges of T_k only) proved unsuccessful, whereas less generous overlapping partitions considering few nodes around Ω_i similarly to the QSEM case cannot be designed straightforwardly, since the internal Fekete nodes are not distributed regularly as in a tensor product.

Overlapping Schwarz preconditioners. Overlapping Schwarz methods can now be described either in matrix form or in terms of a space decomposition of the discrete spaces. Let us consider the matrix form first. The overlapping Schwarz preconditioner B^{-1} for A is based on the following:

(a) the solution of a coarse problem on the coarse mesh τ_0, with bilinear elements for QSEM and bilinear or linear ones for TSEM ($p = 1$);

(b) the solutions of local problems on the overlapping subdomains Ω_i'.

For the coarse solve, we need to define:

(a$_1$) a restriction matrix R_0; its transpose R_0^T interpolates coarse bilinear (resp., bilinear or linear) functions on τ_0 to spectral elements functions on the fine GLL (resp., Fekete) mesh τ_p;

(a$_2$) a coarse stiffness matrix $A_0 = R_0 A R_0^T$ needed for the solution of the coarse problem with $p = 1$ on τ_0.

For the local solves, we need to define the following:

(b$_1$) restriction matrices R_i (with 0,1 entries) returning only the degrees of freedom inside each subdomain Ω_i';

(b$_2$) local stiffness matrices $A_i = R_i A R_i^T$ needed for the solution of the ith local problem on Ω_i' with zero Dirichlet boundary conditions on $\partial\Omega_i'$.

Finally, we define

$$P_i = R_i^T A_i^{-1} R_i A, \qquad i = 0, 1, \ldots, N.$$

These are the building blocks of the proposed preconditioners. The additive form of the overlapping Schwarz preconditioner is

$$(3.1) \quad B_{add}^{-1} = R_0^T A_0^{-1} R_0 + \sum_{i=1}^{N} R_i^T A_i^{-1} R_i, \quad \text{i.e.,} \quad P_{add} \equiv B_{add}^{-1} A = P_0 + \sum_{i=1}^{N} P_i,$$

while the multiplicative form is

$$(3.2) \qquad\qquad B_{mul}^{-1} A = I - (I - P_N) \cdots (I - P_1)(I - P_0).$$

More general hybrid variants can be considered as well; see [28].

These preconditioners are associated with the space decomposition

$$V_{K,p} = V_0 + \sum_{i=1}^{N} V_i,$$

where either $V_{K,p} \equiv V_{K,p}^Q$ or $V_{K,p} \equiv V_{K,p}^T$. Here, V_0 is the subspace of $V_{K,p}$ consisting of piecewise bilinear or linear functions on the coarse mesh τ_0 and for QSEM

$$V_i = \{v \in V_{K,p}^Q : v = 0 \text{ at all the GLL nodes outside } \Omega_i' \text{ and on } \partial\Omega_i'\},$$

while for TSEM

$$V_i = \{v \in V_{K,p}^T : v = 0 \text{ at all the Fekete nodes outside } \Omega_i' \text{ and on } \partial\Omega_i'\}.$$

Defining the operators $T_i : V_{K,p} \longrightarrow V_i, \ i = 0, 1, \ldots, N$, by

$$a_{K,p}(T_i u, v) = a_{K,p}(u, v) \qquad \forall v \in V_i, \ i = 0, 1, \ldots, N,$$

where $a_{K,p} \equiv a_{K,p}^Q$ for QSEM and $a_{K,p} \equiv a_{K,p}^T$ for TSEM, it is then easy to check that $B_{add}^{-1}A$ given in (3.1) is exactly the matrix form of the additive Schwarz operator

$$(3.3) \qquad T_{add} = T_0 + T_1 + \cdots + T_N.$$

Analogously, $B_{mul}^{-1}A$ given in (3.2) is the matrix form of the multiplicative Schwarz operator

$$(3.4) \qquad T_{mul} = I - (I - T_N) \cdots (I - T_1)(I - T_0).$$

Condition number estimates. The spectral equivalence between the QSEM matrices (mass and stiffness) and the usual P_1 finite element matrices obtained when using the GLL nodal mesh (see Casarin [4]) allows us to transfer the main domain decomposition results from the finite element case to QSEM (see, e.g., Toselli and Widlund [32]).

THEOREM 3.1. *The condition number $\kappa_2(T_{add}) = \lambda_{max}(T_{add})/\lambda_{min}(T_{add})$ of the overlapping Schwarz QSEM operator T_{add} in additive form is bounded by*

$$(3.5) \qquad \kappa_2(T_{add}) \leq C\left(1 + \frac{H}{\delta^*}\right),$$

with the constant C independent of p, H, h, δ^*.

As in the standard finite element case, we cannot guarantee that in the case of QSEM this bound is independent of the coefficient jumps in the elliptic operator, in our case α, but the numerical experiments reported in the next section show that such independence holds.

The bound (3.5) implies that in case of minimal overlap $\delta = 1$ GLL points, i.e., $\delta^* \approx h/p^2$, we have

$$(3.6) \qquad \kappa_2(T_{add}) \leq C\left(1 + \frac{H}{h}p^2\right);$$

i.e., the number of iterations is expected to scale like p for fixed H/h, while it scales like $\sqrt{H/h}$ for fixed p. In case of generous overlap $\delta^* = h$, we have

$$(3.7) \qquad \kappa_2(T_{add}) \leq C\left(1 + \frac{H}{h}\right);$$

i.e., the number of iterations is expected to be independent of p and on the order of $\sqrt{H/h}$. This was already proved in Pavarino [23] for hp-finite elements and generous overlap. For unstructured hp elements on nontensorial elements, such as TSEM, the spectral equivalence used for QSEM in [4, 23] does not hold, and preconditioners with small overlap are not known. Nevertheless, we can build preconditioners with generous overlap as shown before, and the numerical results of the next section show that they are optimal and scalable. Hence we conjecture that a bound as in Theorem 3.1 also holds for TSEM.

Complexity estimates for TSEM. We briefly examine here the computational costs of solving both the original TSEM discrete problem and the TSEM preconditioned problem in two dimensions on a serial computer. Analogous estimates can be derived in three dimensions and for QSEM.

We consider for simplicity the square domain $\Omega = (0,1)^2$ with a uniform subdivision in triangular elements as in Figure 3, where the total number of degrees of freedom

is $d_T = O(p^2 N K_i)$, since we have $O(p^2)$ degrees of freedom per element, K_i elements per subdomain, and N subdomains (in this geometry, we have $h^{-1} = \sqrt{N K_i/2}$ and $H^{-1} = \sqrt{N}$). The band of the stiffness matrix is $b_T = O(p^2 \sqrt{N K_i})$, i.e., the number of degrees of freedom on one spectral element row (or column) of the square domain.

(a) The computational cost of solving the original TSEM system with a banded direct solver is $O(d_T b_T^2) = O(p^6 (N K_i)^2)$. The cost of solving the same system with a CG method would be proportional to the number of required CG iterations (i.e., the square root of the condition number $= O(p^2 h^{-1}) = O(p^2 \sqrt{N K_i})$) times the cost of each CG iteration. The latter is dominated by the matrix-vector products, which for our banded matrix involve $O(d_T b_T) = O(p^4 (N K_i)^{3/2})$ operations. Hence the CG cost would be $O(p^6 (N K_i)^2)$, i.e., similar to the direct solver's one.

(b) The computational cost of solving the TSEM system with the Schwartz PCG is again given by the product of the required PCG iterations and the cost of each PCG iteration; see [28, Chapter 3.6]. From (3.7), the condition number of our two-level Schwarz preconditioner with generous overlap is $O(H/h) = O(\sqrt{K_i})$. Since H/h can be kept constant by decreasing h and H proportionally, we have that the PCG iterations are $O(1)$ (otherwise the extra cost would only be a factor $\sqrt{K_i}$). The cost per iteration is dominated by the matrix-vector products and the preconditioner solves. We assume that we have factored the local and coarse matrices before starting the iterations, so that the local and coarse solves are just banded back-substitutions, with band $b_i = O(p^2 \sqrt{K_i})$ for the ith local matrix and band $b_0 = \sqrt{N}$ for the coarse matrix (linear elements on the coarse mesh $\tau_0 = \tau_H$). Denoting by $d_i = O(p^2 K_i)$ and $d_0 = O(N)$ the number of local and coarse degrees of freedom, we have that the cost of the local solves is $O(N d_i b_i) = O(p^4 N K_i^{3/2})$, while the cost of the coarse solve is $O(N^{3/2})$. The overlap costs amount to lower-order terms, since the factor $\sqrt{K_i}$ in the local band b_i is only increased by 1 (if the subdomain touches the domain boundary) or 2 (if the subdomain is internal), and similarly the local number of degrees of freedom d_i is only increased by a factor $O(p^2 \sqrt{K_i})$ corresponding to the elements in the overlapping subregion Ω_i' outside subdomain Ω_i. Adding up the matrix-vector products and all the local and coarse solves of the preconditioner, we then estimate the total PCG cost as $O(p^4 (N K_i)^{3/2} + p^4 N K_i^{3/2} + N^{3/2})$. This cost is lower than the cost of solving the original TSEM system as estimated in (a). Better estimates could be obtained by considering better local and coarse solvers, matrix-vector products, etc. We remark that these serial estimates have a relative importance, since domain decomposition preconditioners should be considered on parallel architectures, where more involved complexity estimates need to include architecture-dependent quantities such as communication and memory costs (see [28, Chapter 3.6]), and are beyond the scope of this paper.

4. Numerical results. We tested the properties of the overlapping Schwarz preconditioned CG method for TSEM and QSEM partitions, by performing a p-, H-, and h-convergence study. We consider either a homogeneous or a heterogeneous material, given by the model problem (2.1) over the domain $\Omega = [-1, 1]^2$. The body force f is consistent with $u(x) = \sin(\pi x)\sin(\pi y)$ as an exact solution of (2.1). The discrete problems are solved by either the CG method or the PCG method, with zero initial guess and stopping criterion $\|\mathbf{r}^{(\nu)}\|_2 / \|\mathbf{b}^{(\nu)}\|_2 \leq 10^{-7}$, where $\mathbf{r}^{(\nu)}$ is the residual of the linear systems $A_T \mathbf{u} = \mathbf{b}$ or $A_Q \mathbf{u} = \mathbf{b}$ at the νth iterate. The Schwarz preconditioner is here applied in the additive version (3.1) without or with the coarse correction given by the term $R_0^T A_0^{-1} R_0$ in (3.1). We recall that the overlapping Schwarz preconditioners are built using generous overlap in the TSEM case and using minimal overlap ($\delta = 1$) in the QSEM case.

TABLE 1

TSEM: iteration counts, condition number, and extreme eigenvalues of the original and preconditioned (with $K_i = 1$) operators, fixing $p = 6$ and varying $1/h = 1/H$. See text for additional explanation.

	CG (no prec.)		PCG without coarse pb.				PCG with coarse pb.			
$1/H$	It.	κ_2	It.	λ_{max}	λ_{min}	κ_2	It.	λ_{max}	λ_{min}	κ_2
2	94	729.37	13	12.99	2.67	4.85	13	12.99	3.35	3.87
3	129	1641.55	14	12.99	1.42	9.14	14	12.99	2.35	5.52
4	161	2916.96	16	12.99	0.84	15.33	15	13.00	1.81	7.16
5	191	4542.20	18	12.99	0.55	23.34	16	13.00	1.53	8.46
6	221	6472.48	21	12.99	0.39	33.15	18	13.00	1.37	9.43
7	248	8470.90	24	12.99	0.23	56.47	19	13.00	1.28	10.15

TABLE 2

TSEM: iteration counts, condition number, and extreme eigenvalues of unpreconditioned and preconditioned (with $K_i = 1$) operators, fixing $N = 4 \times 4 \times 2$ triangular subdomains and varying p.

	CG (no prec.)		PCG without coarse pb.				PCG with coarse pb.			
p	It.	κ_2	It.	λ_{max}	λ_{min}	κ_2	It.	λ_{max}	λ_{min}	κ_2
3	28	84.34	12	12.99	2.66	4.87	13	13.00	3.34	3.88
6	85	729.37	13	12.99	2.67	4.85	13	12.99	3.35	3.87
9	206	4819.90	13	12.99	2.67	4.85	13	12.99	3.35	3.87
12	299	8899.07	13	12.99	2.67	4.85	13	12.99	3.35	3.87
15	456	21738.04	13	12.99	2.67	4.85	13	12.99	3.35	3.87
18	777	49837.97	13	12.99	2.67	4.85	13	12.99	3.35	3.87

4.1. The homogeneous case: The Fekete–Gauss TSEM. In this section, we report the results of numerical experiments for the model problem (2.1) discretized with triangular TSEM using the Fekete and Gauss nodes. We consider a homogeneous material with $\alpha = \beta = 1$.

4.1.1. Case $K_i = 1$. We start with the simple choice of associating each triangular element with a subdomain (i.e., $H = h$, or equivalently, $N = K$). The mesh is obtained by first dividing Ω into M^2 identical squares and then by dividing each of them into two triangles, thus providing a partition of $N = 2M^2$ triangular subdomains. The overlapping partition is described in Figure 2. The grid-size parameter H is equal to $2/M$.

In Table 1, we report the iteration counts (It.), spectral condition number (κ_2), and extreme eigenvalues (λ_{max}, λ_{min}), fixing $p = 6$ and varying the parameter $1/h = 1/H$ from 2 to 7, i.e., varying the number of subdomains from $N = 2 \times 4 \times 4$ to $N = 2 \times 14 \times 14$.

Columns 2–3 refer to unpreconditioned CG, columns 4–7 to PCG without coarse problem, and columns 8–11 to PCG with coarse problem ($\tau_h = \tau_H$ in this case).

The same quantities are reported in Table 2, now fixing $h = H = 1/2$ ($N = 2 \times 4 \times 4$ subdomains) and varying the degree p from 3 to 18.

The condition numbers and extreme eigenvalues (not reported in the tables) of the unpreconditioned Fekete matrix are plotted in Figure 4 as a function of H (left) and p (right). These results show that the very ill-conditioned TSEM original matrix A_T has a condition number that grows as $O(p^4 h^{-2})$. The maximum eigenvalue λ_{max} grows as $O(p^2)$, and $1/\lambda_{min}$ grows as $O(p^2 h^{-2})$. The results also show that the overlapping Schwarz preconditioned operator with or without coarse solver is optimal in p, since all the quantities are bounded by constants independent of p (Table 2). Without the coarse problem the preconditioner loses its scalability (Table 1), since
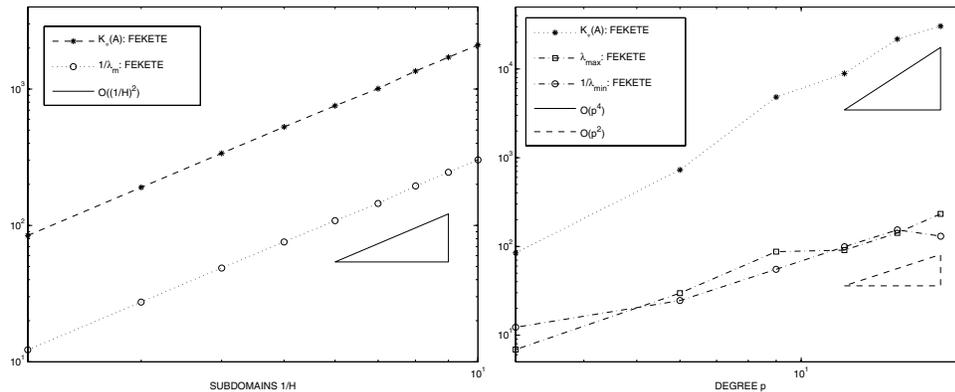
FIG. 4. *TSEM: log-log plot of the condition number of the unpreconditioned Fekete operator as a function of $h = H$ (left) and p (right) from the data of Tables* 1 *and* 2.

λ_{min} tends to 0 with increasing N, while the addition of a coarse problem seems to guarantee scalability (higher values of $1/H$ would be necessary in order to clearly asses scalability).

4.1.2. Case $K_i > 1$. We now consider the more general case where each subdomain Ω_i contains several triangular elements. The TSEM partition is built by first dividing the square computational domain Ω into $N = M^2$ identical square subdomains Ω_i, with $M = 2, \ldots, 6$. Then a fine local partition is considered within each subdomain, consisting of $2 \times 2, \ldots, 6 \times 6$ smaller squares, each of them being divided into two identical triangular elements, so that $K_i = 8, 18, \ldots, 72$. Each subdomain Ω_i is then extended into an overlapping subdomain Ω_i' by adding all the surrounding elements that intersect its boundary; see Figure 3(left). The numerical results with the overlapping Schwarz preconditioner are obtained with both the τ_h-coarse space and τ_H-coarse space.

First, we check the convergence properties of our TSEM preconditioners with respect to the number of subdomains, fixing $p = 6$ as total degree of the polynomials within each triangle and with $h = H/3$. The results are reported in Table 3 and plotted in Figure 5(left). As expected, one observes an increase of the condition number when no coarse solver is used. However, nice results are obtained when the preconditioner employs either one of the τ_h- or τ_H-coarse spaces, and the condition number appears to be bounded above by a constant of about 20.

Second, we vary the number K_i of triangular elements in each subdomain; i.e., we vary the ratio H/h. The results are reported in Table 4 and plotted in Figure 6(left). Again, one observes the efficiency of the overlapping Schwarz preconditioner, especially when a coarse solver is included. Here it should be remarked that the result is better than expected, since the condition number appears to be independent of H/h, i.e., K_i.

Third, we vary the TSEM polynomial degree p. The results are reported in Table 5 and plotted in Figure 7(left). Of course, the coarse solver has no influence here, and all the three preconditioners have slowly increasing condition numbers that seem to be bounded above by a constant independent of p. We note that such slow increase toward an upper bound was not observed in the case $K_i = 1$ (Table 2), where the independence of p was very clear.

TABLE 3

TSEM: iteration counts, condition number, and extreme eigenvalues of the original and pre-conditioned matrix, fixing $p = 6$, $K_i = 3 \times 3 \times 2$, and varying N.

	CG			PCG	without coarse pb.		
N	It.		κ_2	It.	λ_{max}	λ_{min}	κ_2
2×2	129		1641.54	37	7.81	0.43	18.07
3×3	176		3687.55	39	8.52	0.38	21.99
4×4	221		6471.91	47	8.71	0.22	39.36
5×5	261		9348.38	46	7.87	0.15	49.95
6×6	329		12152.89	54	7.52	0.11	64.86
	PCG	with τ_h-coarse pb.		PCG	with τ_H-coarse pb.		
N	It.	λ_{max}	λ_{min}	κ_2	It.	λ_{max}	λ_{min}	κ_2
2×2	37	7.82	0.43	18.13	37	7.81	0.43	18.12
3×3	37	8.54	0.45	18.67	37	8.52	0.45	18.66
4×4	40	8.72	0.43	19.85	41	8.72	0.44	19.89
5×5	37	7.94	0.45	17.42	37	7.87	0.45	17.30
6×6	37	7.55	0.45	16.53	39	7.52	0.45	16.60
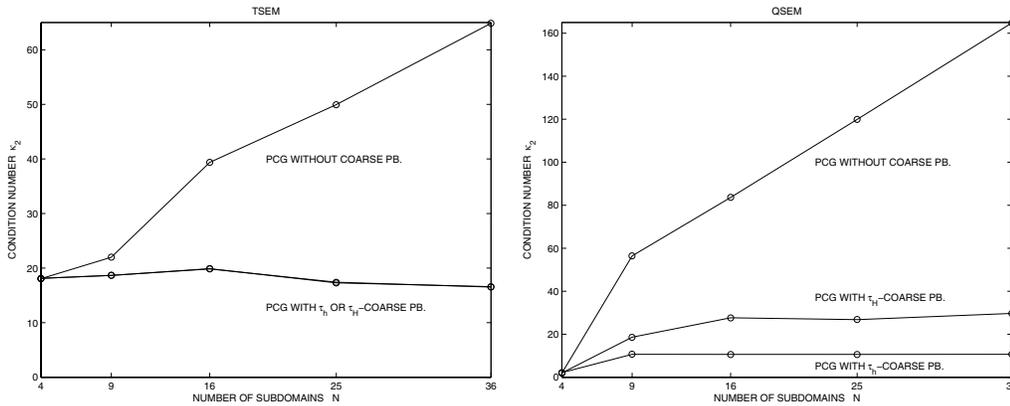
FIG. 5. *Condition number of PCG with and without coarse problem as a function of the number of subdomains N; TSEM data from Table 3 (left), QSEM data from Table 6 (right).*

These results show that the overlapping Schwarz preconditioner with a coarse problem is optimal and scalable also in the nontrivial case $H \neq h$, i.e., $K_i > 1$. The results are not as clear as in the trivial case with only one element per subdomain ($H = h$, i.e., $K_i = 1$), but we conjecture that numerical experiments with higher values of p and N would confirm these properties.

4.2. The homogeneous case: The GLL QSEM. Overlapping Schwarz methods for QSEM based on GLL points have been successfully applied to many elliptic and parabolic problems (see, e.g., [32, 7] and the references therein). Numerical results are usually carried out by considering the simpler choice $H = h$ with only one element per subdomain.

In this section, we report the results of numerical experiments with GLL QSEM for the same tests and model problem (2.1) of the previous section. We focus on the nontrivial case $H \neq h$ and perform analogous p-, H-, and h-convergence tests. The QSEM partition is built by dividing the square computational domain Ω into $N = M^2$ identical square subdomains Ω_i of characteristic diameter H. Then a local partition is considered within each subdomain, consisting of K_i square elements of

TABLE 4

TSEM: iteration counts, condition number, and extreme eigenvalues of the original and preconditioned matrix, fixing $p = 6$, $N = 3 \times 3$, and varying K_i.

| K_i	CG It.			κ_2	PCG It.	without coarse pb. λ_{max}	λ_{min}	κ_2
$2 \times 2 \times 2$	129			1641.54	36	8.48	0.45	18.54
$2 \times 3 \times 3$	176			3687.55	39	8.52	0.38	21.99
$2 \times 4 \times 4$	221			6471.91	40	7.88	0.28	27.34
$2 \times 5 \times 5$	261			9348.38	47	8.49	0.21	40.17
$2 \times 6 \times 6$	329			12152.89	48	8.53	0.18	46.14
K_i	PCG It.	with τ_h-coarse pb. λ_{max}	λ_{min}	κ_2	PCG It.	with τ_H-coarse pb. λ_{max}	λ_{min}	κ_2
$2 \times 2 \times 2$	36	8.49	0.45	18.54	36	8.48	0.46	18.47
$2 \times 3 \times 3$	37	8.54	0.45	18.67	37	8.52	0.45	18.66
$2 \times 4 \times 4$	36	7.95	0.46	17.27	37	7.88	0.45	17.20
$2 \times 5 \times 5$	38	8.50	0.45	18.60	39	8.49	0.45	18.61
$2 \times 6 \times 6$	38	8.54	0.45	18.69	40	8.53	0.45	18.69
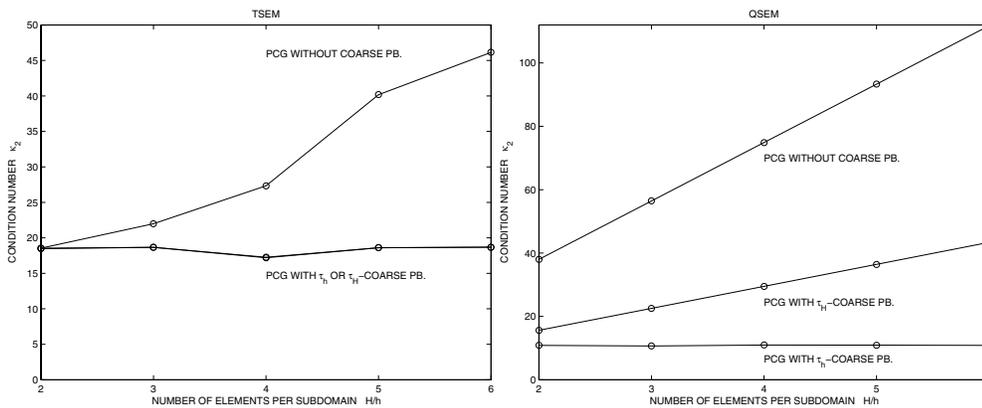
FIG. 6. *Condition number of PCG with and without coarse problem as a function of the number of elements per subdomain H/h; TSEM data from Table 4 (left), QSEM data from Table 7 (right).*

TABLE 5

TSEM: iteration counts, condition number, and extreme eigenvalues of the original and preconditioned matrix, fixing $N = 3 \times 3$, $K_i = 2 \times 3 \times 3$, and varying p.

| p	CG It.			κ_2	PCG It.	without coarse pb. λ_{max}	λ_{min}	κ_2
3	59			428.10	32	6.88	0.38	17.78
6	176			3687.55	39	8.52	0.38	21.99
9	437			24235.35	43	9.39	0.38	24.23
12	625			44816.79	45	9.81	0.38	25.30
15	940			109050.07	47	10.03	0.38	25.88
18	1460			236603.08	48	10.16	0.38	26.22
p	PCG It.	with τ_h-coarse pb. λ_{max}	λ_{min}	κ_2	PCG It.	with τ_H-coarse pb. λ_{max}	λ_{min}	κ_2
3	29	7.13	0.55	12.89	30	6.89	0.55	12.50
6	37	8.54	0.45	18.67	37	8.52	0.45	18.66
9	41	9.39	0.42	22.12	42	9.39	0.42	22.23
12	43	9.81	0.41	23.41	44	9.81	0.41	23.65
15	45	10.03	0.41	24.10	46	10.04	0.41	24.39
18	46	10.16	0.41	24.47	47	10.16	0.40	24.80
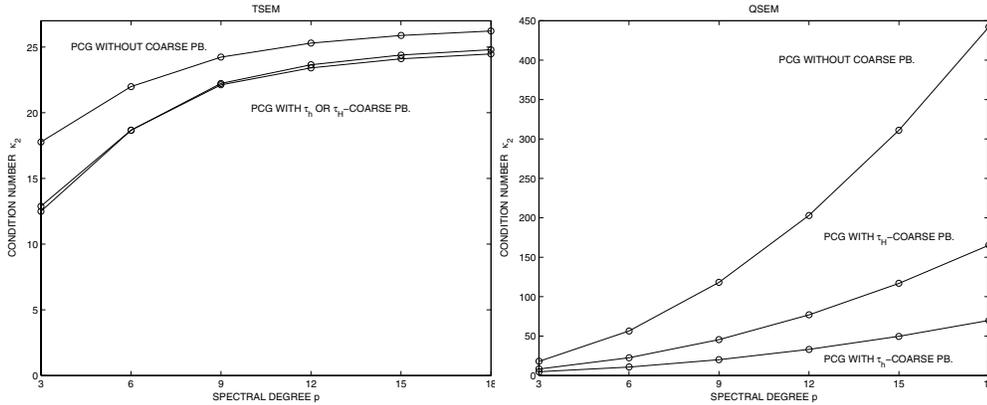
FIG. 7. *Condition number of PCG with and without coarse problem as a function of the spectral degree p; TSEM data from Table* 5 *(left), QSEM data from Table* 8 *(right).*

TABLE 6

QSEM: iteration counts, condition number, and extreme eigenvalues of the original and pre-conditioned matrix, fixing $p = 6$, $K_i = 3 \times 3$, minimal overlap $\delta = 1$, and varying N.

N	CG It.			κ_2	PCG It.	without coarse pb. λ_{max}	λ_{min}	κ_2
2×2	67			270.78	8	1.93	1.00	1.93
3×3	106			603.09	25	4.00	0.07	56.45
4×4	141			1067.56	30	4.00	0.05	83.60
5×5	175			1667.71	41	4.00	0.03	119.93
6×6	213			2399.75	46	4.00	0.02	164.83
N	PCG It.	with τ_h-coarse pb. λ_{max}	λ_{min}	κ_2	PCG It.	with τ_H-coarse pb. λ_{max}	λ_{min}	κ_2
2×2	10	2.17	1.00	2.17	8	2.00	1.00	2.00
3×3	20	4.01	0.37	10.68	23	8.52	0.45	18.66
4×4	21	4.01	0.38	10.62	27	4.00	0.14	27.68
5×5	22	4.01	0.38	10.65	32	4.00	0.15	26.80
6×6	22	4.01	0.37	10.69	33	4.00	0.13	29.70

characteristic diameter h, and a tensorial GLL mesh is introduced in each element. We then extend each subdomain Ω_i to an overlapping subdomain Ω_i' with minimal overlap, consisting of just $\delta = 1$ layer of GLL nodes outside the boundary; see Figure 1(right) and section 3.

We first study the convergence properties of overlapping Schwarz preconditioners for QSEM with respect to the number of subdomains. We compare the overlapping Schwarz preconditioner operator based either on the τ_h- or the τ_H-coarse space. In Table 6 we report the same quantities of the previous section, and we plot them in Figure 5(right). We fix the local polynomial degree $p = 6$ and the number of elements per subdomain $K_i = 3 \times 3$, which corresponds to $H = 3h$, varying the number of subdomains from $N = 2 \times 2$ to $N = 6 \times 6$. While both unpreconditioned CG and PCG without coarse problem are not scalable, PCG with either the τ_h- or τ_H-coarse space is.

We then consider the convergence properties with respect to the number K_i of elements per subdomain in Table 7 and plot the results in Figure 6(right). We fix the local polynomial degree $p = 6$ and the number of subdomains $N = 3 \times 3$, varying the number of elements per subdomain from $K_i = 2 \times 2$ to $K_i = 6 \times 6$. In agreement

TABLE 7

QSEM: iteration counts, condition number, and extreme eigenvalues of the original and pre-conditioned matrix, fixing $p = 6$, $N = 3 \times 3$, minimal overlap $\delta = 1$, and varying K_i.

K_i	CG It.			κ_2	PCG It.	without coarse pb. λ_{max}	λ_{min}	κ_2
2×2	67			270.78	20	4.00	0.10	38.03
3×3	106			603.09	25	4.00	0.07	56.45
4×4	141			1067.56	29	4.00	0.05	74.88
5×5	175			1667.71	32	4.00	0.04	93.31
6×6	213			2399.75	34	4.00	0.03	111.74
K_i	PCG It.	with τ_h-coarse pb. λ_{max}	λ_{min}	κ_2	PCG It.	with τ_H-coarse pb. λ_{max}	λ_{min}	κ_2
2×2	19	4.01	0.37	10.86	19	4.00	0.26	15.63
3×3	20	4.01	0.37	10.68	23	4.00	0.18	22.55
4×4	21	4.01	0.36	10.97	26	4.00	0.13	29.49
5×5	21	4.01	0.37	10.92	30	4.00	0.11	36.43
6×6	21	4.01	0.37	10.84	32	4.00	0.09	43.38

TABLE 8

QSEM: iteration counts, condition number, and extreme eigenvalues of the original and pre-conditioned matrix, fixing $N = 3 \times 3$, $K_i = 3 \times 3$, minimal overlap $\delta = 1$, and varying p.

p	CG It.			κ_2	PCG It.	without coarse pb. λ_{max}	λ_{min}	κ_2
3	46			118.29	15	4.00	0.22	17.89
6	106			603.10	25	4.00	0.07	56.45
9	178			1627.80	35	4.00	0.03	118.18
12	263			3553.80	45	4.00	0.02	203.07
15	359			6707.30	55	4.00	0.01	311.11
18	464			11379.62	65	4.00	0.01	442.30
p	PCG It.	with τ_h-coarse pb. λ_{max}	λ_{min}	κ_2	PCG It.	with τ_H-coarse pb. λ_{max}	λ_{min}	κ_2
3	14	4.09	0.85	4.81	15	4.02	0.49	8.23
6	20	4.01	0.37	10.68	23	4.00	0.18	22.55
9	27	4.00	0.20	20.11	32	4.00	0.09	45.50
12	33	4.00	0.12	33.14	41	4.00	0.05	76.96
15	41	4.00	0.08	49.75	50	4.00	0.03	116.90
18	48	4.00	0.06	69.91	58	4.00	0.02	165.32

with the theoretical estimate of Theorem 3.1, the preconditioner with the τ_H-coarse space yields condition numbers that grow linearly with K_i. On the other hand, the τ_h-coarse space yields condition numbers that are independent of K_i.

We then study the convergence properties with respect to the polynomial degree p in Table 8 and plot the results in Figure 7(right). We fix the number of subdomains $N = 3 \times 3$, and the number of elements per subdomain $K_i = 3 \times 3$, varying the local polynomial degree from $p = 3$ to $p = 18$. In agreement with the bound of Theorem 3.1, all PCG iteration counts display a linear growth with p, corresponding to a quadratic growth of the condition number associated with a quadratic decay of λ_{min} (while λ_{max} has a constant value of about 4).

Finally, we consider the convergence properties of our preconditioner with respect to the overlap δ (number of GLL points extending Ω_i in each direction) in Table 9 and plot the same results with respect to the corresponding values of δ^* (size of the overlapping region) in Figure 8. We fix the number of subdomains $N = 3 \times 3$, the number of elements per subdomain $K_i = 2 \times 2$, the local polynomial degree $p = 9$, varying the overlap from $\delta = 1$ GLL points (minimal overlap) to $\delta = 9$ GLL

TABLE 9
QSEM: iteration counts, condition number, and extreme eigenvalues of P_{add}, fixing $N = 3 \times 3$, $K_i = 2 \times 2$, $p = 9$, and varying the overlap δ. Columns 2–5 refer to the coarse mesh $\tau_0 \equiv \tau_H$, and columns 6–9 refer to the richer coarse mesh $\tau_0 \equiv \tau_h$.

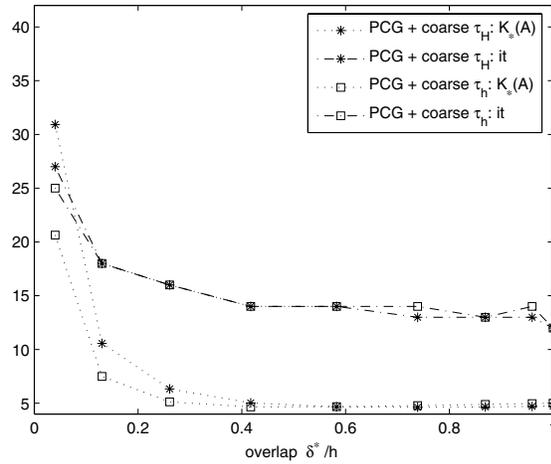|	PCG with τ_H-coarse pb.				PCG with τ_h-coarse pb.			
δ	It.	λ_{max}	λ_{min}	κ_2	It.	λ_{max}	λ_{min}	κ_2
1	27	4.00	0.13	30.92	25	4.00	0.19	20.64
2	18	4.02	0.38	10.57	18	4.04	0.54	7.49
3	16	4.08	0.64	6.34	16	4.16	0.81	5.13
4	14	4.20	0.83	5.04	14	4.36	0.94	4.66
5	14	4.35	0.93	4.67	14	4.58	0.98	4.68
6	13	4.50	0.97	4.63	14	4.77	1.00	4.77
7	13	4.62	0.99	4.66	13	4.89	1.00	4.89
8	13	4.70	1.00	4.70	14	4.97	1.00	4.97
9	12	4.74	1.00	4.74	12	5.00	1.00	5.00

FIG. 8. *QSEM: condition number and iteration counts for the overlapping Schwarz preconditioned operator, as a function of the overlap size δ^* normalized with respect to h, from the corresponding data expressed in terms of δ in Table 9.*

points (generous overlap). Again in agreement with the theory, the condition numbers improve with increasing δ because λ_{min} improves considerably. The improvement is large in going from $\delta = 1$ to $\delta = 2$ and 3, while it becomes rapidly marginal (or negative) for larger values of δ, due to the slight growth of λ_{max}.

4.3. The heterogeneous case: The Fekete–Gauss TSEM. To check the efficiency of the additive Schwarz preconditioner for TSEM, we vary the diffusion coefficient α in the elliptic operator of our model problem (2.1). The computations are done for the reference case with $p = 6$, $N = 3 \times 3$, and $K_i = 2 \times 3 \times 3$.

First, we use two different values of α, $\alpha_1 = 1$ in some subdomains and $\alpha_2 = 10^t$, with $t = -3, -2, \ldots, 3$ in the others. These two values are distributed in a checkerboard layout on the subdomains, starting with α_1 on the top left subdomain; see Figure 9(left). The results are reported in Table 10. We remark that the efficiency of the overlapping Schwarz preconditioner is not affected by the jump of α at the interfaces of the subdomains, while unpreconditioned CG greatly suffers the severe

1	10^t	1
10^t	1	10^t
1	10^t	1

10	10^{-2}	10^5
10^4	10^6	1
10^{-3}	10^2	10^{-1}

FIG. 9. *Values of the discontinuous coefficient α of the elliptic operator in the heterogeneous test of Tables 10 and 11: checkerboard (left) and random (right) layout.*

TABLE 10

TSEM for heterogeneous case: iteration counts, condition number, and extreme eigenvalues of the original and preconditioned matrix, fixing $p = 6$, $K_i = 3 \times 3 \times 2$, $N = 3 \times 3$, and considering the coefficient α discontinuous across subdomains.

	CG				PCG	without coarse pb.		
t	It.			κ_2	It.	λ_{max}	λ_{min}	κ_2
−3	1023			31023.64	41	9.45	0.45	20.70
−2	798			16120.09	41	9.42	0.45	20.61
−1	387			8493.16	40	9.16	0.45	20.07
0	176			3687.55	39	8.52	0.38	21.99
1	443			8689.35	38	8.43	0.45	18.48
2	1164			49766.04	39	9.07	0.45	19.84
3	3058			285022.32	40	9.17	0.45	20.08
Random	*			*	49	9.46	0.40	23.58
	PCG	with τ_h-coarse pb.			PCG	with τ_H-coarse pb.		
t	It.	λ_{max}	λ_{min}	κ_2	It.	λ_{max}	λ_{min}	κ_2
−3	40	9.46	0.45	20.61	40	9.45	0.45	20.69
−2	40	9.43	0.45	20.49	41	9.42	0.45	20.59
−1	39	9.17	0.45	20.00	40	9.16	0.45	20.06
0	37	8.54	0.45	18.67	37	8.52	0.45	18.66
1	38	8.52	0.45	18.65	38	8.43	0.45	18.48
2	39	8.79	0.45	19.27	40	8.80	0.45	19.30
3	41	8.84	0.45	19.40	41	8.86	0.45	19.45
Random	48	9.47	0.45	20.64	50	9.46	0.45	20.74

ill-conditioning of the problems due to the increasing coefficient jumps.

We then consider a harder case with "random" distribution of α shown in Figure 9(right), and report the results in the last line of Table 10. Even in this very difficult case, where unpreconditioned CG does not seem to converge, the overlapping Schwarz preconditioner remains very efficient.

4.4. The heterogeneous case: The GLL QSEM. Analogous conclusions are obtained with GLL QSEM; see Table 11. Here the condition numbers of the preconditioned operator seem to even improve with increasing coefficient jumps, while their maximum is attained in absence of jumps for $t = 0$. For the difficult test case with the same random distribution of α, unpreconditioned CG again fails to converge, while the overlapping Schwarz preconditioner requires about the same iterations as in absence of jumps.

5. Conclusions. We have constructed and studied overlapping Schwarz preconditioners for the triangular/tetrahedral spectral element (TSEM) discretization of scalar elliptic problems based on Fekete nodes. The proposed preconditioners employ generous overlap among subdomains, since it is not currently know how to construct TSEM preconditioners with small overlap. We also compared the TSEM nontensorial

TABLE 11

QSEM: iteration counts, condition number, and extreme eigenvalues of the original and precon-ditioned matrix, fixing $p = 6$, $K_i = 3 \times 3$, $N = 3 \times 3$, and considering the coefficient α discontinuous across subdomains.

	CG			PCG	without coarse pb.		
t	It.		κ_2	It.	λ_{max}	λ_{min}	κ_2
-3	631		18069	11	4.00	0.60	6.65
-2	390		6576	14	4.00	0.46	8.76
-1	207		1445	19	4.00	0.16	25.01
0	106		603.10	25	4.00	0.07	56.45
1	241		2958.20	19	4.00	0.17	22.79
2	669		27712	13	4.00	0.47	8.58
3	>1000		275540	11	4.00	0.60	6.65
Random	*		*	24	4.00	0.03	114.17
	PCG	with τ_h-coarse pb.		PCG	with τ_H-coarse pb.		
t	It.	λ_{max}	λ_{min}	κ_2	It.	λ_{max}	λ_{min}	κ_2
-3	14	4.01	0.90	4.46	13	4.00	0.82	4.88
-2	15	4.01	0.78	5.13	15	4.00	0.66	6.07
-1	17	4.01	0.50	8.02	20	4.00	0.30	13.29
0	20	4.01	0.37	10.68	23	4.00	0.18	22.55
1	16	4.01	0.59	6.82	18	4.00	0.36	10.94
2	13	4.01	0.85	4.73	14	4.00	0.68	5.85
3	12	4.01	0.90	4.45	12	4.00	0.79	5.02
Random	23	4.01	0.45	8.84	25	4.00	0.32	12.59

discretization with the classical Gauss–Lobatto–Legendre QSEM discretization, where it is possible to construct Schwarz preconditioners with variable overlap (from gener-ous to minimal). In spite of the more severe ill-conditioning of the resulting TSEM discrete problem (where $\kappa_2 \approx O(p^4 h^{-2})$), the convergence rate of the proposed pre-conditioning algorithm is independent of the number of subdomains N when a coarse problem is employed and of the spectral degree p in case of generous overlap; other-wise it depends inversely on the overlap size. Moreover, the proposed preconditioners are robust with respect to arbitrary jumps across subdomains of the coefficients of the elliptic operator. Our results are limited to regular structured meshes in the plane. Future work will extend this study to three dimensions and to unstructured meshes for more general domains.

REFERENCES

[1] C. Bernardi and Y. Maday, *Spectral methods*, in Handbook of Numerical Analysis, Volume V, Techniques of Scientific Computing (Part 2), North–Holland, Amsterdam, 1997, pp. 209–485.

[2] I. Bica, *Iterative Substructuring Methods for the p-Version Finite Element Method for Elliptic Problems*, Ph.D. thesis, Courant Institute, New York University, New York, 1997; technical report 1997-743.

[3] L. Bos, M. A. Taylor, and B. A. Wingate, *Tensor product Gauss–Lobatto points are Fekete points for the cube*, Math. Comp., 70 (2001), pp. 1543–1547.

[4] M. A. Casarin, *Quasi-optimal Schwarz methods for the conforming spectral element discretiza-tion*, SIAM J. Numer. Anal., 34 (1997), pp. 2482–2502.

[5] Q. Chen and I. Babuška, *Approximate optimal points for polynomial interpolation of real functions in an interval and in a triangle*, Comput. Methods Appl. Mech. Engrg., 128 (1995), pp. 485–494.

[6] Q. Chen and I. Babuška, *The optimal symmetrical points for polynomial interpolation of real functions in a tetrahedron*, Comput. Methods Appl. Mech. Engrg., 137 (1996), pp. 89–94.

[7] M. O. Deville, P. F. Fischer, and E. H. Mund, *High-Order Methods for Incompressible Fluid Flow*, Cambridge University Press, London, 2002.

[8] M. DRYJA AND O. B. WIDLUND, *Domain decomposition algorithms with small overlap*, SIAM J. Sci. Comput., 15 (1994), pp. 604–620.

[9] M. DUBINER, *Spectral methods on triangles and other domains*, J. Sci. Comput., 6 (1991), pp. 345–390.

[10] P. F. FISCHER, *An overlapping Schwarz method for spectral element solution of the incompressible Navier–Stokes equations*, J. Comput. Phys., 133 (1997), pp. 84–101.

[11] P. F. FISCHER AND J. W. LOTTES, *Hybrid Schwarz–multigrid methods for the spectral element method: Extensions to Navier–Stokes*, J. Sci. Comput., 6 (2005), pp. 345–390.

[12] F. X. GIRALDO AND T. WARBURTON, *A nodal triangle-based spectral element method for the shallow water equations on the sphere*, J. Comput. Phys., 207 (2005), pp. 129–150.

[13] F. X. GIRALDO, *High-order triangle-based discontinuous Galerkin methods for hyperbolic equations on a rotating sphere*, J. Comput. Phys., 214 (2006), pp. 447–465.

[14] J. S. HESTHAVEN, *From electrostatics to almost optimal nodal sets for polynomial interpolation in a simplex*, SIAM J. Numer. Anal., 35 (1998), pp. 655–676.

[15] J. S. HESTHAVEN AND C. H. TENG, *Stable spectral methods on tetrahedral elements*, SIAM J. Sci. Comput., 21 (2000), pp. 2352–2380.

[16] J. S. HESTHAVEN AND T. WARBURTON, *Nodal high-order methods on unstructured grids*, J. Comput. Phys., 181 (2002), pp. 186–221.

[17] G. E. KARNIADAKIS AND S. J. SHERWIN, *Spectral/hp Element Methods for Computational Fluid Dynamics*, 2nd ed., Oxford University Press, London, 2005.

[18] A. KLAWONN AND L. F. PAVARINO, *Overlapping Schwarz methods for mixed linear elasticity and Stokes problems*, Comput. Meth. Appl. Mech. Engrg., 165 (1998), pp. 233–245.

[19] R. PASQUETTI AND F. RAPETTI, *Spectral element methods on triangles and quadrilaterals: Comparisons and applications*, J. Comput. Phys., 198 (2004), pp. 349–362.

[20] R. PASQUETTI AND F. RAPETTI, *Spectral element methods on unstructured meshes: Comparisons and recent advances*, J. Sci. Comput., 27 (2006), pp. 377–387.

[21] R. PASQUETTI, L. F. PAVARINO, F. RAPETTI, AND E. ZAMPIERI, *Overlapping Schwarz preconditioners for Fekete spectral elements*, in Domain Decomposition Methods in Science and Engineering 16, O. B. Widlund and D. Keyes, eds., Lecture Notes in Comput. Sci. Engrg. 55, Springer, New York, 2006, pp. 717–724.

[22] R. PASQUETTI, F. RAPETTI, L. F. PAVARINO, AND E. ZAMPIERI, *Neumann–Neumann–Schur complement methods for Fekete spectral elements*, J. Engrg. Math., 56 (2006), pp. 323–335.

[23] L. F. PAVARINO, *Additive Schwarz methods for the p-version finite element method*, Numer. Math., 66 (1994), pp. 493–515.

[24] L. F. PAVARINO AND T. WARBURTON, *Overlapping Schwarz methods for unstructured spectral elements*, J. Comput. Phys., 160 (2000), pp. 298–317.

[25] L. F. PAVARINO AND E. ZAMPIERI, *Overlapping Schwarz and spectral element methods for linear elasticity and elastic waves*, J. Sci. Comput., 27 (2006), pp. 51–73.

[26] A. QUARTERONI AND A. VALLI, *Domain Decomposition Methods for Partial Differential Equations*, Oxford Science Publications, London, 1999.

[27] C. SCHWAB, *p- and hp-Finite Element Methods. Theory and Applications in Solid and Fluid Mechanics*, Oxford University Press, New York, 1998.

[28] B. F. SMITH, P. BJØRSTAD, AND W. D. GROPP, *Domain Decomposition: Parallel Multilevel Methods for Elliptic Partial Differential Equations*, Cambridge University Press, London, 1996.

[29] B. SZABÓ AND I. BABUŠKA, *Finite Element Analysis*, John Wiley & Sons, New York, 1991.

[30] M. A. TAYLOR, B. A. WINGATE, AND R. E. VINCENT, *An algorithm for computing Fekete points in the triangle*, SIAM J. Numer. Anal., 38 (2000), pp. 1707–1720.

[31] M. A. TAYLOR AND B. A. WINGATE, *A generalized diagonal mass matrix spectral element method for nonquadrilateral elements*, Appl. Numer. Math., 33 (2000), pp. 259–265.

[32] A. TOSELLI AND O. B. WIDLUND, *Domain Decomposition Methods: Algorithms and Theory*, Comput. Math. 34, Springer-Verlag, Berlin, 2004.

[33] T. WARBURTON, L. F. PAVARINO, AND J. S. HESTHAVEN, *A pseudo-spectral scheme for the incompressible Navier–Stokes equation using unstructured nodal elements*, J. Comput. Phys., 164 (2000), pp. 1–21.